



Deposited via The University of Sheffield.

White Rose Research Online URL for this paper:

<https://eprints.whiterose.ac.uk/id/eprint/215568/>

Version: Published Version

Article:

Houghton, R.J. and Goodwin, S.P. (2024) From cores to stars: searching for a universal rule for star formation. *Monthly Notices of the Royal Astronomical Society*, 531 (3). pp. 3373-3385. ISSN: 0035-8711

<https://doi.org/10.1093/mnras/stae1364>

Reuse

This article is distributed under the terms of the Creative Commons Attribution (CC BY) licence. This licence allows you to distribute, remix, tweak, and build upon the work, even commercially, as long as you credit the authors for the original work. More information and the full terms of the licence here:

<https://creativecommons.org/licenses/>

Takedown

If you consider content in White Rose Research Online to be in breach of UK law, please notify us by emailing eprints@whiterose.ac.uk including the URL of the record and the reason for the withdrawal request.

From cores to stars: searching for a universal rule for star formation

Rebecca J. Houghton ★ and Simon P. Goodwin

Department of Physics and Astronomy, The University of Sheffield, Hounsfield Rd, Sheffield S3 7RH, UK

Accepted 2024 May 10. Received 2024 May 10; in original form 2023 March 11

ABSTRACT

Star formation is generally considered to be ‘universal’, meaning that it is statistically the same everywhere (and at all times). We investigate whether it is possible to find a simple rule for the conversion of molecular cores into bound stellar systems, along with the resulting secular decay and dynamical destruction of these systems, which can match the field initial mass functions (IMFs) and multiplicity statistics. We find that extreme cases, in which the core fragmentation is self-similar or has a strong dependence on initial core mass, cannot reproduce the observations of the field. However, a model in which core fragmentation is fairly weakly dependent on core mass has some success, if we include the effects of secular decay on the multiplicity statistics. This model both fits the IMF well and has an overabundance of low-mass binary systems over the field that matches local star-forming regions. However, it is unclear whether this overabundance could be dynamically processed to match the field.

Key words: methods: statistical – binaries: general – stars: formation.

1 INTRODUCTION

How stars form is one of the most important questions in astrophysics. The physics behind star formation is extremely complex, involving self-gravity, magnetohydrodynamics, thermal physics, and chemistry in a turbulent medium. Our best observation of the outcome of star formation is the field, which is the sum of many different star formation events in different parts of the Galaxy, spread over a long period of time. The initial mass function (IMF) in the field and in nearby clusters has been extensively studied (see reviews by Bastian, Covey & Meyer 2010; Kroupa et al. 2013; Offner et al. 2014). The results of such studies can be used to determine whether each star formation event produces statistically very similar outcomes (that are each not too different from the field), or whether different star formation events are very different, and the field is just an average over all the ways in which star formation can occur (Goodwin 2010).

It is important to know what the spread of star formation outcomes is for a number of reasons. When we perform a simulation of star formation (attempting to include a wide variety of physics), how do we know whether we have the ‘right’ answer? Should a simulation always produce an outcome not too dissimilar to the field, or could simulations with varying initial conditions that produce very different results all be correct? Answering these questions can tell us whether there is a simple initial input into e.g. population synthesis models, or whether we need to start with a wide variety of initial subpopulations. It also allows us to investigate the environmental dependence of star formation.

If all star formation events are roughly similar and produce something not too different from the field, then it would seem like much of the complexity of the physics of star formation should in some way ‘average out’. That is, if different giant molecular clouds (GMCs) of different masses and density distributions, with

different levels of turbulence, magnetic field geometries, external radiation fields, and chemistry and metallicity, all produce very similar outcomes in terms of the stars they produce, then this might argue for a fairly simple set of ‘rules’ that describe star formation.

In this paper, we start from the assumptions that (a) stellar masses are set by observed core masses and (b) all star formation produces something like the field. If these are both true, then there may well be some ‘simple rule’ of star formation. We are not arguing that these assumptions are correct; they merely represent the assumptions we wish to test.

The two most useful observations of the field that we would want to fit with a toy star formation model are the IMF and multiplicity properties. If all star formation produces something similar to the field, then all star formation events should produce an IMF and multiplicity properties like those we observe in the field.

The IMF of stars seems usually to be ‘universal’, in particular in local, resolved stellar populations (Bastian et al. 2010; Offner et al. 2014), which might suggest that star formation is always similar (at least in how it distributes mass between stars). Furthermore, observations of the core mass function (CMF) in star-forming regions indicate that this is also universal, with a similar shape to the IMF but shifted to higher masses (see e.g. Könyves et al. 2020, and references therein). Determining IMFs is a difficult task, especially in young regions (see the discussion in Offner et al. 2014). However, they can be determined with sufficient accuracy that the general consensus is that IMFs in different regions are broadly similar to each other and to the field.

If the IMFs of different regions are always similar, this could be taken to argue that the mechanism by which stars accumulate mass is always the same. There are two main theories on how stars gather mass (we summarize them here, but see Offner et al. 2014, for a much more detailed discussion).

Stars form from molecular cores, which themselves have a CMF (as observed by Könyves et al. 2010, 2015). Therefore, the IMF and CMF must bear some relation to each other. The simplest of such

* E-mail: astro.rhoughton@gmail.com

theories suggests that the stellar masses are directly inherited from the CMF (Padoan & Nordlund 2002; Hennebelle & Chabrier 2008; Holman et al. 2013). However, the link between the CMF and the IMF is complex; for example, the CMF is a measure of the current masses of cores, whereas we are interested in the mass available for stars, which may change due to accretion, interactions with protostellar systems, or turbulence (i.e. Bonnell, Larson & Zinnecker 2007; Bate 2012; Offner et al. 2014; Pelkonen et al. 2021). It is worth noting that even in simple CMF–IMF models such as ours we require the cores to lose mass to fit to the IMF, which we include as a star formation efficiency (SFE).

The reason we take the simple assumption that the CMF maps simply to the IMF is that we want also to address another observation of the field as well as the IMF – multiplicities. Two interesting observations are that the multiplicity of field stars seems to increase significantly with primary mass (Offner et al. 2023, and references therein) and local star-forming regions appear to have higher multiplicities than the field (Kraus et al. 2011; King et al. 2012a, b; Duchêne et al. 2018).

Studies of the field mean that we have a clear picture of the distribution of multiplicities by primary mass (Offner et al. 2023, and references therein), along with the IMF. We also know that stars form in single and/or multiple systems from gravitationally bound dense cores (e.g. Sadavoy & Stahler 2017), but multiple systems can decay through secular (e.g. Sterzik & Durisen 1998; Delgado-Donate, Clarke & Bate 2003; Valtonen et al. 2008; Reipurth & Mikkola 2012) or dynamical processes (e.g. Parker & Goodwin 2012; Rawirawattana & Goodwin 2023). This leads to two basic theories of how the field is produced: (1) stars form with multiplicities similar to the field or (2) stars form with much higher multiplicities and decay to produce the field values (e.g. Kroupa 1995a, b). It is more likely that the true process is a combination of both theories, rather than a result of either of the two extremes.

A particularly interesting feature of the multiplicity properties of the field is that all measures of multiplicity increase significantly over a small range of mass. Low-mass stars are almost all single, while high-mass stars are almost all in (higher order) multiples. The change from low multiplicity to high multiplicity occurs between primary masses of approximately 0.5 and 5 M_{\odot} , with 1 M_{\odot} being the ‘mid-point’. This range of masses does not seem to correspond to any feature in the IMF (the peak being at much lower masses).

In this paper, we test various probabilistic/statistical Monte Carlo models for how cores split into stars, and how the resulting systems decay. The aim of these models is to see whether a set of simple rules can be used to find a simple, ‘universal’ model of star formation (i.e. one that reproduces the IMF and multiplicities of the field). As we shall see, we do struggle to find such a model, although we do find a model that does an arguably reasonable job.

2 BACKGROUND

2.1 The CMF and the IMF

The IMF has been determined for many different regions, using stellar evolution theories and mass–age–luminosity relations to convert between the observed luminosity function (LF) and the mass function (MF). The IMF has been fitted with several functional forms, which are an approximately lognormal/power-law slope at low masses, a turnover at ~ 0.1 – $0.2 M_{\odot}$, and a high-mass power-law slope of $\Gamma = -2.35$ (Salpeter 1955; Kroupa 2001; Chabrier 2003; Maschberger 2013). Although there are occasionally slight differences in the shape of the IMF depending on the environment

(Bastian et al. 2010), the high-mass power slope, turnover at 0.1–1.0 M_{\odot} , and lognormal/power-law slope for low masses appear to be universal features (Chabrier 2003; Guszejnov & Hopkins 2015).

The CMF has also been studied in various star-forming regions using molecular tracers (Benson & Myers 1989; Scibelli & Shirley 2020) and dust continuum mapping (Motte, Andre & Neri 1998; André et al. 2010; Könyves et al. 2010; Marsh et al. 2016; Massi et al. 2019) to identify dense cores. The CMFs determined through these studies appear to have an approximately lognormal shape (André et al. 2010), with a high-mass slope with an exponent of $\Gamma = -2.35$ and a peak mass of around $\sim 1 M_{\odot}$.

The similarities between the CMF and the IMF are often taken to imply a direct and self-similar mapping between the two functions, where the IMF is shifted to lower masses by a factor of ~ 3 – 5 (Motte et al. 1998; Padoan & Nordlund 2002; Alves, Lombardi & Lada 2007; Nutter & Ward-Thompson 2007; Könyves et al. 2010; Guszejnov & Hopkins 2015). The shift in the peak of the IMF is therefore assumed to be proportional to the SFE (η) of dense cores, implying a value of ~ 30 per cent. This matches both observations and simulations (Alves et al. 2007; Goodwin et al. 2008; Könyves et al. 2015; Marsh et al. 2016), which determine values of ~ 20 – 40 per cent.

The physical mechanisms responsible for the relationship between the CMF and the IMF are still unclear. Often it is assumed that the CMF is in some sense static, and hence shows the reservoirs of gas available to individual stellar systems. However, it is not clear whether this is the case and several models propose that core growth via accretion from the surrounding molecular cloud is crucial, and stellar masses are not determined solely by the material contained in a pre-stellar core at the instant it is observed (e.g. Bonnell & Bate 2006; Vázquez-Semadeni et al. 2019; Nony et al. 2023). We will assume the CMF is static and directly responsible for the IMF, but it is not clear whether this assumption is true.

If all stars in multiple systems could be resolved perfectly, then the observed IMF would be the single-star IMF. However, as many stars are in multiples that cannot be resolved, there is also the system IMF (the IMF of the combined mass of all stars in a bound stellar system). Both the system and single-star IMFs have been parametrized by Chabrier (2003) and Maschberger (2013). As we will discuss, it is doubtful we ever actually observe the system IMF as many higher order systems will decay on a very short time-scale, and any system mass function observed in the field has (at least partially) been dynamically processed. Throughout we will use the phrase ‘system IMF’ for convenience, to distinguish the mass function from the multiplicity fraction, MF.

It should be noted that field MFs and the IMFs of young systems are rather uncertain with incompleteness, unresolved companions, and model-dependent mass determinations (especially for pre-main-sequence stars) creating possibly significant ‘error bars’ on any mass function determination.

2.2 Multiplicity fractions

Many stars are observed in multiple systems, and must form as multiples as their dynamical creation is extremely unlikely in almost all environments we observe.

Multiple systems are thought to be formed through core fragmentation and/or disc fragmentation. Simulations show that core fragmentation is often induced by turbulence and radiative feedback, with larger amounts of turbulence potentially leading to more fragmentation, and therefore higher order multiple systems (Goodwin, Whitworth & Ward-Thompson 2004; Attwood et al. 2009; Bate 2012; Lomax et al. 2015; Guszejnov, Hopkins & Krumholz 2017;

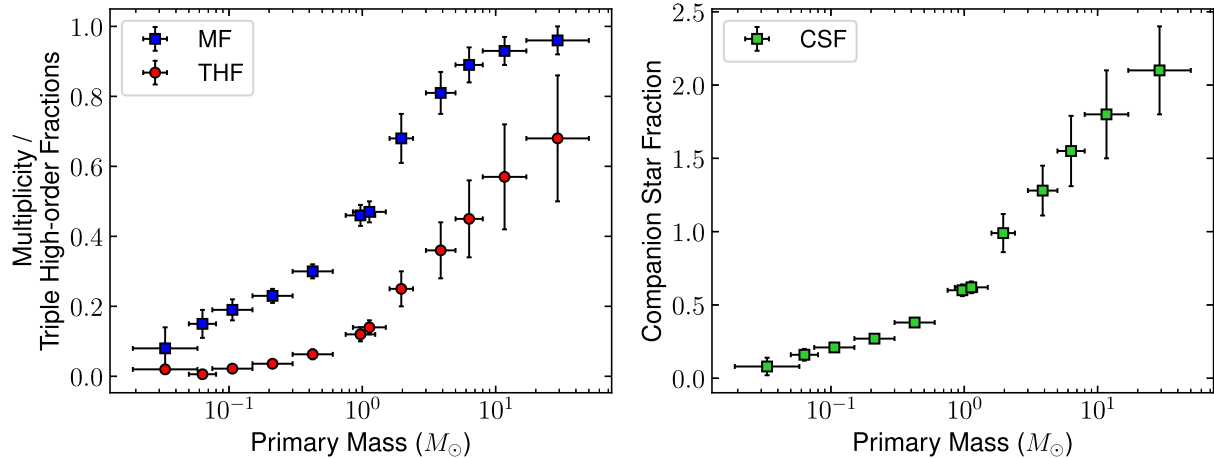


Figure 1. The MFs (blue squares, left), THFs (red circles, left), and CSFs (green squares, right) for various primary mass ranges. The x -error bars represent the total mass range sampled for which the MF/THF is calculated. All points are corrected for incompleteness. Adapted from Offner et al. (2023), using the values from their table 1.

Chen et al. 2020). Disc fragmentation predominantly occurs in massive discs around intermediate and higher mass stars, and is believed to increase the MFs at higher masses (Kratter & Lodato 2016, and references therein). If one mechanism is more important than the other is unclear, and one might think that their relative importance should depend on the system/primary mass and/or the general environment. In our models, we just provide a simple rule for fragmentation and do not consider exactly how this happens.

Stellar multiplicity is commonly quantified using the multiplicity fraction, MF (i.e. the fraction of primaries with at least one companion),

$$\text{MF} = \frac{B + T + Q + \dots}{S + B + T + Q + \dots}, \quad (1)$$

where S , B , T , and Q are the numbers of single, binary, triple, and quadruple systems of a given spectral type, respectively. Similarly, the fraction of triple or higher order systems is given by the triple/higher order fraction (THF),

$$\text{THF} = \frac{T + Q + \dots}{S + B + T + Q + \dots}, \quad (2)$$

and the average number of companions per primary star is given by the companion star fraction (CSF),

$$\text{CSF} = \frac{B + 2T + 3Q + \dots}{S + B + T + Q + \dots}. \quad (3)$$

The MF, THF, and CSFs found in various observational surveys are shown in Fig. 1. We see that the MF depends strongly on the mass of the primary star, ranging from ~ 20 per cent for M dwarfs (Fischer & Marcy 1992; Ward-Duong et al. 2015; Winters et al. 2019) to ~ 50 per cent for solar-type stars (Duquennoy & Mayor 1991; Raghavan et al. 2010; Tokovinin 2014) up to ≥ 80 per cent for massive stars (Mason et al. 2009; Sana et al. 2012; De Rosa et al. 2014; Sana et al. 2014; Moe & Di Stefano 2017). The THF and CSFs also imply that the majority of high-mass stars will be in triple or higher order systems.

Observationally determined MFs suffer from systematic uncertainties due to incompleteness corrections (i.e. unresolved companions), and Malmquist bias if the sample is magnitude limited. The multiplicity statistics in Fig. 1 are corrected for biases and incompleteness.

Observations of nearby star-forming regions show a significantly higher number of multiples compared to the field (Leinert et al. 1993; Duchêne 1999; Haisch et al. 2004; Duchêne & Kraus 2013; Duchêne et al. 2018; Tobin et al. 2022). However, this is primarily the case for associations rather than dense clusters (Duchêne et al. 2018), as clusters typically have similar multiplicities to the field (Patience et al. 2002; Deacon & Kraus 2020; Torres, Latham & Quinn 2021). This could be explained if almost all stars form in multiple systems (Goodwin & Kroupa 2005) and then undergo significant post-formation processing due to a combination of both secular (from inherent instabilities and without external perturbations) and dynamical (from encounters with other stars in dense environments and star-forming regions) decay, which lowers the MFs and results in the field population (Goodwin et al. 2007). This would imply a universal method of star formation and environment-dependent decay (Kroupa & Bouvier 2003).

3 THE MODEL

Our key question is: Can we find a very simple set of rules that takes us from the CMF to both the stellar and system IMFs and the field multiplicities? To investigate this, we use Monte Carlo simulations, where we define a simple rule for the way cores are split into stars (representing the fragmentation process), and assign some probability that a system decays (representing the combined effects of both dynamical and secular decay). An ideal model will be able to produce a canonical IMF, and also replicate the increase of the MF/CSFs with primary mass.

We compare the results of our simulations to the *overall* MFs determined through each survey, rather than the binary fraction over a particular separation range. This is because in our simple model we do not produce separations at all (doing so would require several extra parameters and take us away from our goal of trying to be as simple as possible).

Our results show that it is difficult to find a model that replicates these trends, and it is unclear whether a simple rule exists.

3.1 Simulations

All simulations begin by drawing masses for n cores (with masses M_c) from the Maschberger function (Maschberger 2013). Our CMF

adopted the characteristic parameters of the L_3 system IMF, but with a scale parameter (i.e. peak value) of $1 M_\odot$, a lower mass limit of $m_l = 0.1 M_\odot$, and an upper mass limit of $m_u = 150 M_\odot$. For all simulations presented in Section 4, the number of cores sampled was set at $n = 1 \times 10^6$.

Each core then fragments into N_* stars, where the N_* can be random or vary with mass. We discuss the rules we use to fragment cores in detail in Section 4, as it turns out that these are crucial when trying to match the observations. Note that although we refer to the cores as fragmenting into a defined number of stars, this represents the sum of processes such as classical core fragmentation or via disc fragmentation, as the nature of our simulations means that the microphysical properties of the core are not modelled.

The total stellar mass, M_{sys} , is calculated using the core mass multiplied by the SFE, η , so $M_{\text{sys}} = \eta M_c$. As discussed in Section 2.1, a single efficiency factor is often assumed due to the mapping between the CMF and the IMF. To rectify the fact that a constant value of η might not be representative of the efficiency in all scenarios, such as high-mass stars continuing to accrete (i.e. Pelkonen et al. 2021; Nony et al. 2023), we ran several simulations with different values of η .

In the first, η is assumed to be constant. In the second, η varies randomly between 0 and 1 for each core. One might expect the SFE to vary systematically, depending on the mass of the embedded stars (Matzner & McKee 2000). However, it is not clear whether this would increase (due to more gas contained within the larger potential well of the star) or decrease (due to stellar feedback) the SFE with increasing core mass (Goodwin et al. 2008). Since we are aiming to find an overall rule for explaining the origin of the field population, a constant value of the SFE should represent an average of the SFE across all cores.

The total stellar mass is then divided up between the stars by randomly selecting $N_* - 1$ mass ratio values q from a uniform distribution in the range 0.2–1. For binary systems, we select a single value of q_{12} and assign masses such that $m_2 = q_{12}m_1$. For triple systems, m_3 will have the value $q_{23}m_2$. This pattern is continued for higher order systems. This gives initial mass-ratio distributions (pre-dynamical and secular processing) similar to those of the field (cf. Goodwin 2013).

3.2 Secular decay and dynamical destruction

The steps above produce an initial system, containing either a single or multiple stars. However, if the initial system is a multiple, there is a possibility that it will not enter the field in its initial state; higher order multiples can decay due to secular effects, and systems can be dynamically destroyed by an encounter. Decay and destruction alter the multiplicity statistics, and change the system IMF (note that the single-star IMF is not altered by decay and destruction).

Secular decay should (to a first approximation) be environment independent, but the efficiency of destruction depends on the density and velocity dispersion of the environment of a system that sets the frequency and energy of encounters that could destroy a system (Hurley, Aarseth & Shara 2007; Parker & Goodwin 2012).

The field represents the sum of star formation across all environments over all time. If star formation is universal in the sense that there is some ‘typical outcome’, we might hope that a single, simple rule could capture both the secular decay and dynamical destruction of (initially statistically identical) populations to give the field multiplicities. Therefore, we try to use a single probability distribution of a system ‘decaying’ to represent the combined effects

Table 1. The decay probabilities for $N = 2-7$ systems. The column headings show the different decay channels defined according to Sterzik & Durisen (1998), where BS: binary system and $N - 2$ singles; TS: triple system and $N - 3$ singles; QS: quadruple system and $N - 4$ singles; BBS: two binary systems and $N - 4$ singles; and TB: one triple system and one binary system and $N - 5$ singles. The $N = 3, 4,$ and 5 rows contain the values from Sterzik & Durisen (1998) (for a clump mass spectrum), and the other rows (in bold) contain the extrapolated values for lower/higher order systems based on these probabilities.

N	BS	TS	QS	BBS	TB	Other
2	1000	–	–	–	–	–
3	874	118	–	–	–	8
4	751	181	37	12	–	19
5	532	340	62	41	8	17
6	313	499	87	70	31	–
7	94	658	112	99	37	–

of both dynamic and secular decay. As we will discuss throughout Section 4, such a rule struggles to match observations.

For the simplest combined model, each channel of decay for a system of N_* stars is mass independent and has an equal probability; This leads to a scenario where 50 per cent of binaries ‘decay’ to two singles and 50 per cent remain stable. For triples, one-third of systems will eject two stars, one-third will eject one star, and the rest will remain stable. Similarly, for quadruples, one-quarter of systems will eject one star, one-third of systems will eject two stars, etc. This pattern continues for $N_* = 5$ and $N_* = 6$. As we expect the lowest mass objects to be preferentially lost (at least in secular decay; Anosova 1986; Reipurth & Mikkola 2012; Reipurth et al. 2014), we remove stars and make them single in order of increasing mass.

Due to the high rate of decay of binaries, these probabilities are representative of a population that has a high rate of destruction due to interaction with other stars (Parker & Goodwin 2012), and are a good starting point for testing the effect of different overall decay rates on MFs.

However, in reality, it is unlikely that all decay channels have equal probability. Sterzik & Durisen (1998) give probabilities for different decay channels, and include channels that our simple rules do not (such as the decay of a quadruple to a pair of binaries, see Table 1). However, this only accounts for secular decay, not dynamical destruction. We return to these points in much more detail later.

3.3 Output

We use the stellar masses outputted from our simulations to calculate the stellar IMF, to compare with the canonical IMF. We compute both the single-star IMF (the IMF counting all stars) and the system IMF (using the mass of each stellar system M_{sys}).

We also calculate the multiplicity statistics of our stellar population for different primary mass intervals. Due to the fact that all observed multiplicity values used for comparison are corrected for incompleteness, all companions with a mass greater than $0.012 M_\odot$ (\sim minimum brown dwarf mass) are included in our statistics. This is discussed further in Section 5.2.

The output of our simulations provides the multiplicity statistics and IMF at the end stage of star formation, when the systems are dynamically evolved and dispersed into the field.

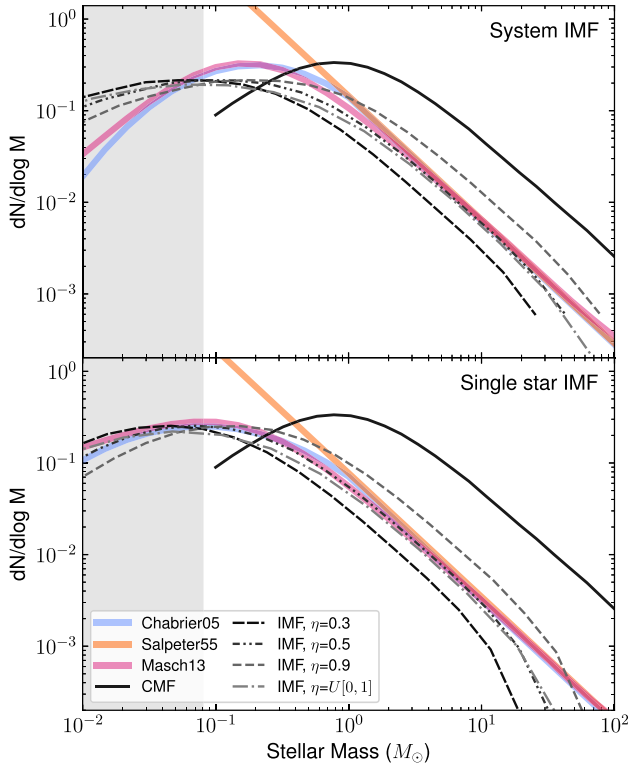


Figure 2. The system (top) and single-star (bottom) IMFs for the fully random model. On both plots, the Salpeter (orange), Chabrier (blue), and Maschberger (pink) IMFs are shown by the solid lines. (The functional forms of the Salpeter and Chabrier IMFs were generated using <https://github.com/keflavich/imf>.) The CMF used in our simulations is shown by the solid black line. The IMFs are plotted for several values of the SFE: $\eta = 0.3$ (densely dashed), $\eta = 0.5$ (dotted), $\eta = 0.9$ (dashed), and $\eta = U[0, 1]$ (dash-dotted). The grey-shaded region on the left of both plots shows the brown dwarf regime.

4 RESULTS

4.1 Self-similar model

We start with a set of models in which all cores fragment into a random number of stars between N_{\min} and N_{\max} , with no dependence on the initial core mass (as used as the basis for simulations such as Goodwin et al. 2008; Holman et al. 2013). The reason why models such as this were used by Goodwin et al. (2008) and Holman et al. (2013) is that they are self-similar and so preserve the shape of the CMF in the IMF, with some combination of fragmentation and SFE shifting the peak of the distribution. Therefore we expect this model to give a good fit to the IMF.

We repeat this simulation with several fixed values of the SFE (η) and one scenario where η is allowed to vary randomly between cores.

For the simulations we present, we assume that *all* cores form multiple systems with $N_{\min} = 2$ and $N_{\max} = 6$ with no dependence on core mass. We use our simple combined decay model to then evolve these initial multiple systems.

In Figs 2, 3, and 4, we show the system and stellar IMFs, multiplicity properties, and mass-ratio distributions, respectively, of one particular simulation. This simulation is representative of every self-similar simulation and the problems they all face in trying to fit the data.

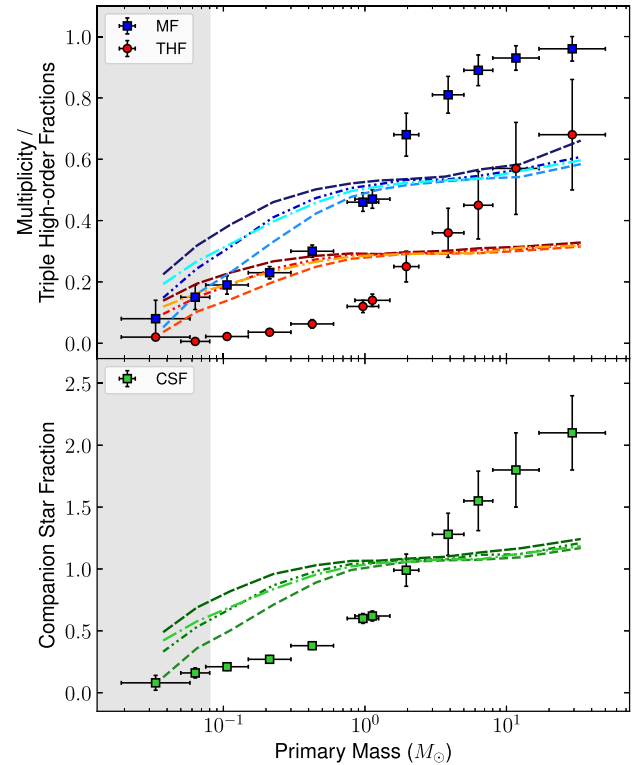


Figure 3. Top: Observed MFs (blue squares) and THFs (red circles) from various sources listed in table 1 of Offner et al. (2023). The blue lines and red lines show the MFs and THFs, respectively, from our model using random fragmentation and ejection rules. The values for the MFs and THFs are plotted for several values of the SFE: $\eta = 0.3$ (densely dashed), $\eta = 0.5$ (dotted), $\eta = 0.9$ (dashed), and $\eta = U[0, 1]$ (dash-dotted). Bottom: CSFs following the same rules as the top plot.

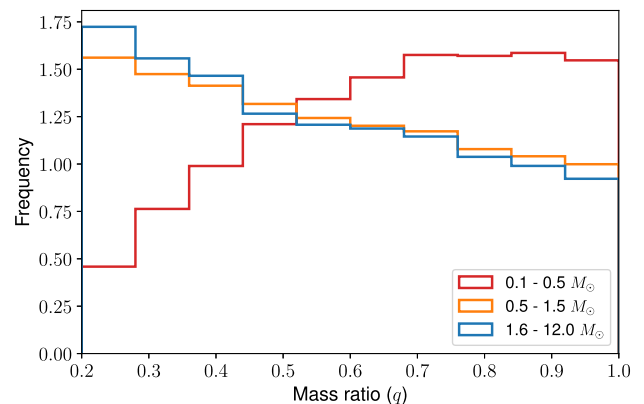


Figure 4. Mass-ratio distributions for systems with M-type primaries (~ 0.1 – $0.5 M_{\odot}$, red), solar-type primaries (~ 0.55 – $1.45 M_{\odot}$, orange), and A/B type primaries (~ 1.6 – $12.0 M_{\odot}$, blue) for the self-similar model. The data are normalized for better comparison between the three mass ranges. These values do not include any brown dwarf companions.

Fig. 2 shows the resulting IMFs from our simulations in comparison to the normalized Salpeter (Salpeter 1955) in orange, Chabrier (Chabrier 2003) in blue, and Maschberger (Maschberger 2013) in pink, forms of the IMF. The top plot of Fig. 2 shows the system IMF and the bottom plot shows the single-star IMF (both after processing).

The CMF is shown by the solid black line, and the dashed black lines are the system and single-star IMFs for different values of the SFE.

The single-star IMFs are a very good fit to the canonical IMFs. This is unsurprising as this model was designed to produce this match by preserving the shape of the CMF. The system IMFs are significantly wider than the canonical system IMFs; while this could possibly be fixed by adjusting how masses are distributed between stars within a core, there seems very little point due to the poor fit of the multiplicities.

Fig. 3 shows the fit from this model to the multiplicity properties of stars. The blue points and red points in the top plot show the observed MFs and THFs, respectively, and the green points in the bottom plot show the observed CSFs (from table 1 of Offner et al. 2023). The horizontal error bars show the primary mass interval covered by each data point. The various dashed blue, red/orange, and green lines on each plot represent our MFs, THFs, and CSFs, respectively, for the same discrete mass ranges as the Offner et al. (2023) values, but shown as a continuous line to aid the eye.

The most obvious thing about Fig. 3 is what a poor fit the model is to the data. All observed multiplicity measures increase with primary mass and rise sharply in the mass range 0.5–5 M_{\odot} . However, the simulations rise slowly from very low masses and plateau above around 1 M_{\odot} .

The details of this behaviour are down to the details of our model, especially the decay probabilities, but they are indicative of a significant problem with this general self-similar model. If all cores produce multiple systems, then for *all* masses the initial (pre-decay and dynamical destruction) population will have the same, very high multiplicity measures (MF = 1, THF \sim 1, and a CSF > 1). We expect higher order systems to decay that produces single stars so diluting the multiplicities, but roughly equally at all masses (because the lowest mass objects are ejected there is a slight tendency to dilute low-mass multiplicities more). Therefore, using a self-similar fragmentation model with mass/multiplicity-independent decay probabilities leads to a roughly flat multiplicity–mass dependency, which completely fails to match the observations. This issue is present regardless of the values used for N_{\min} and N_{\max} and actually flattens the multiplicity–mass dependence further if cores are allowed to form a single star, as shown in Fig. 5. This contradicts findings from multiplicity studies such as Tobin et al. (2022), revealing a fundamental flaw in the assumptions of this model.

In Fig. 4, we show the mass-ratio distributions for M-type stars, solar-type stars, and intermediate/high-mass stars. To fit the observations, we would expect the mass-ratio distribution for M stars to be skewed towards equal mass ratios, solar-type stars to be approximately flat, and intermediate/high-mass stars skewed towards more unequal mass-ratio distributions (Offner et al. 2023, and references therein). Whilst the low-mass stars appear to follow the observed trend, there is little distinction between the mass ratios in the 0.5–1.5 M_{\odot} range and the 1.6–12.0 M_{\odot} range.

Again, this is a result of the self-similar nature of this model, where the multiplicity does not depend on the initial mass of the core. As the MFs are approximately the same for masses \gtrsim 1 M_{\odot} , the mass-ratio distributions will not differ significantly for primaries within this mass range. Changing the way in which masses are distributed between the stars in our model may improve the mass ratios, but would not fix the issues with the MFs and would break the self-similarity.

In this model, we have essentially applied a flat dynamical decay probability with mass to systems that survive secular decay. This

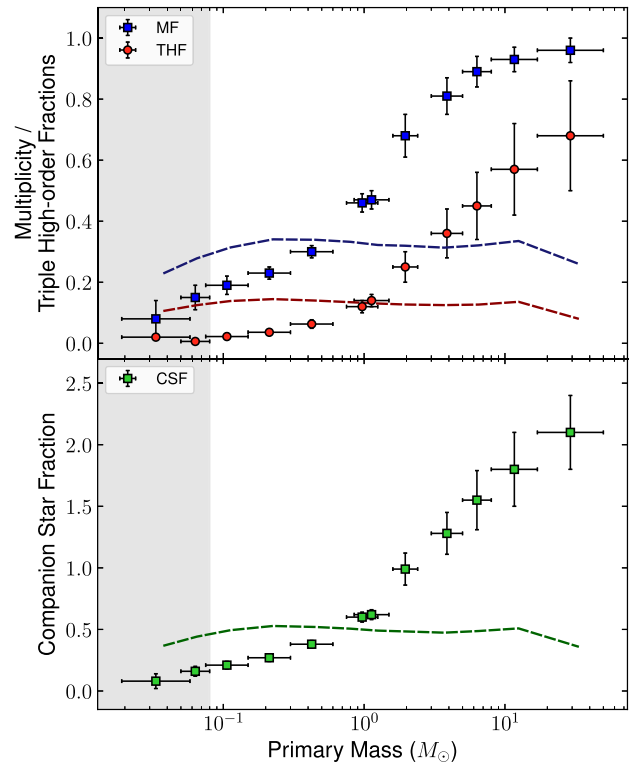


Figure 5. MFs (top, blue dashed line), THFs (top, red dashed line), and CSFs (bottom, green dashed line) for the self-similar model simulation where the number of stars formed varies between one star ($N_{\min} = 1$) and a maximum of four stars ($N_{\max} = 4$). This simulation used an SFE value of $\eta = 0.3$, but is characteristic of the results for all different efficiencies. The blue, red, and green points are as defined in the caption for Fig. 2.

probability has to be extremely high to try and reduce the low-mass multiplicities to close to the observed values, which (as can be seen in Fig. 3) then reduces the high-mass multiplicities to well below the observations.

One can imagine a dynamical decay probability that depends on mass (which is more physical – higher mass systems should be more resistant to dynamical decay), but it would need to be a very strong function of mass. Systems $> 5 M_{\odot}$ need to survive, while almost all systems $< 0.5 M_{\odot}$ need to be destroyed, with a ‘tipping point’ at $\sim 1 M_{\odot}$ where there is a 50 per cent survival chance. Such a dynamical decay function would seem rather fine-tuned, and it is not obvious why destruction would be so tuned to primary mass. There are various scenarios where dynamical decay is thought to be common (e.g. Kroupa 1995a), but that requires low-mass stars to all be born in environments where decay is probable, which seems unlikely [e.g. the review of Wright et al. (2022) suggests a significant fraction of stars are born in associations].

To summarize, a mass-independent fragmentation of cores gives a good fit to the IMF by design, but produces at best only a very weak correlation between mass and multiplicity, which is not what is observed. Whilst there may be scenarios that produce a strong decay–mass relationship, they would need to be very fine-tuned and go against the purpose of this paper, which is to investigate if there are *simple*, universal rules that take us from a CMF to the observed IMF(s) and multiplicity properties.

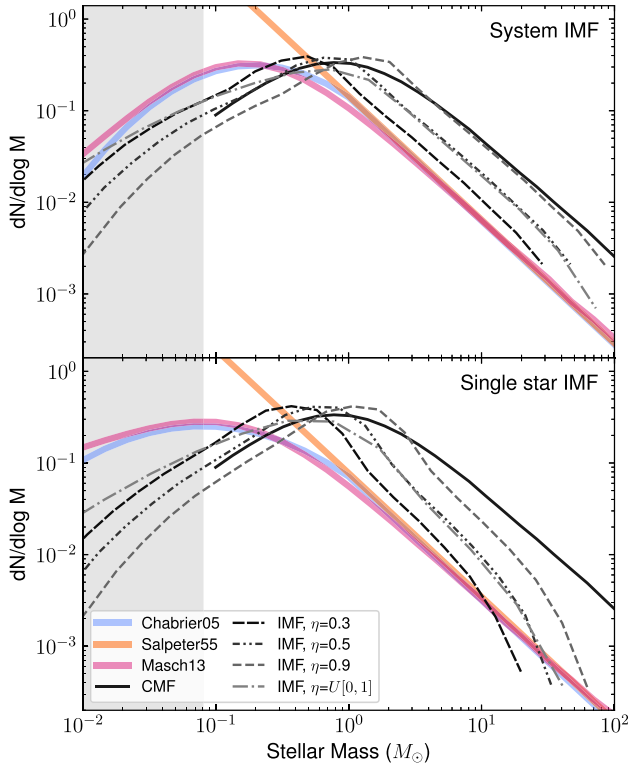


Figure 6. IMFs from the BE mass-dependent model. See the caption for Fig. 2 for more details.

4.2 Strongly mass-dependent model

We showed above that self-similar fragmentation of cores produces multiplicities that are much too flat with respect to mass. Therefore, it is possible that a better match to the multiplicities could be found if N_* increases with M_c .

Some theories suggest that the number of stars formed from a collapsing core may be proportional to the ratio of the core mass to the critical Bonnor–Ebert (BE) mass M_{BE} (e.g. Lada et al. 2008), which is the maximum mass that can be contained within an isothermal BE sphere while remaining in hydrostatic equilibrium (Ebert 1955; Bonnor 1956). In general, M_{BE} is given by

$$M_{BE} = 1.82 \left(\frac{\bar{n}}{10^4 \text{ cm}^{-3}} \right)^{-0.5} \left(\frac{T}{10 \text{ K}} \right)^{1.5} M_{\odot}, \quad (4)$$

where \bar{n} is the volume density of the core, and T is the temperature (Lada et al. 2008). M_{BE} is often represented in terms of parameters such as the external pressure, density, or speed of sound in the medium. Due to its dependence on the properties of the host cloud, the critical BE mass varies significantly depending on the host environment, e.g. from $\sim 0.6 M_{\odot}$ in the Aquila cloud (Könyves et al. 2015) up to $\sim 2 M_{\odot}$ in the Pipe Nebula (Lada et al. 2008). We discuss below the possible implications of this variation.

We consider a case in which the multiplicity of the final system is a strong function of the initial core mass, with each core fragmenting such that $N_* = M_c/M_{BE}$. For the results presented in this section, we randomly select a value of the critical BE mass from a uniform distribution between 0.5 and $2.5 M_{\odot}$.

Figs 6, 7, and 8 show the IMFs, multiplicities, and mass-ratio distributions from this model (cf. Figs 2, 3, and 4 above).

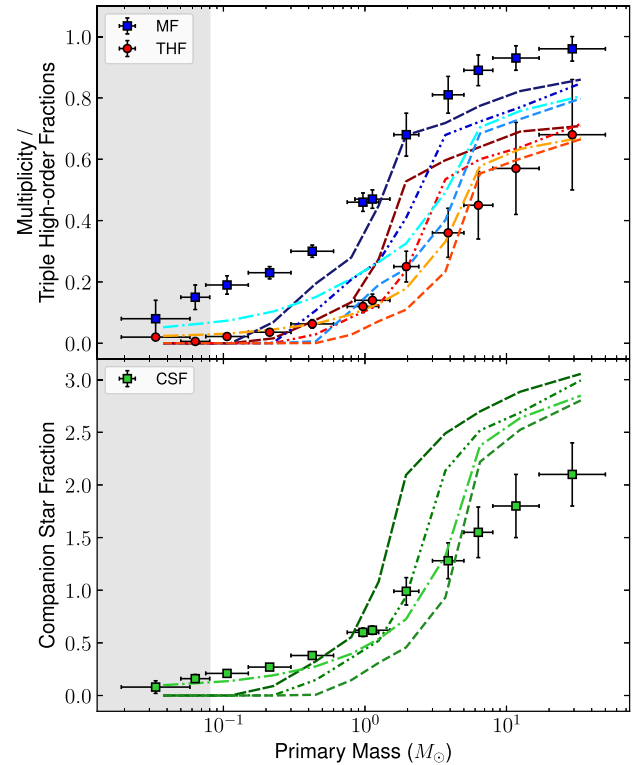


Figure 7. Multiplicities from the BE mass-dependent model. See the caption for Fig. 3 for more details.

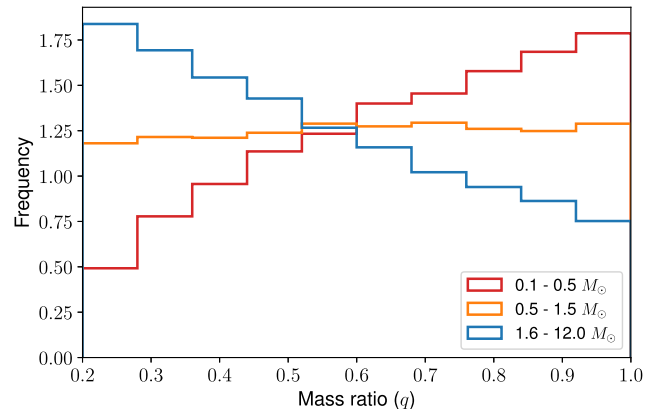


Figure 8. Mass-ratio distributions for the BE mass-dependent model, using a value for the SFE that varies from a random uniform distribution between cores. See the caption for Fig. 4 for more details.

As expected, the multiplicities in Fig. 7 now show a strong dependence on primary mass, comparable with the observed dependence. The THFs show a reasonable fit to the observations and although the MFs are far from a perfect fit, it captures the fundamental trends well. Similarly, the mass-ratio distributions now show a much stronger distinction between their trends for different mass ranges, showing the characteristically flat distribution for solar-type stars and skewed distributions for high- and low-mass stars.

However, there is a significant flaw in this model when it comes to the multiplicities: due to the condition that all stars below the BE mass do not form stars, and cores below $2M_{BE}$ form only one

star, multiple systems with a total mass of less than $2\eta M_{\text{BE}}$ cannot form. As soon as the core mass exceeds M_{BE} , we see a huge jump in the multiplicity as suddenly cores start forming two or more stars. As N_* increases with M_c , the MF, THF, and CSF all continue to increase rapidly as the core mass exceeds two BE masses. Therefore, this model does manage to approximate the multiplicity statistics for stars $>1 M_\odot$, but fails at producing low-mass binaries. It is worth noting that the mass-ratio distributions in Fig. 8 now follow the trends that we expect from the observations, but small variations in the SFE cause the mass-ratio distributions to vary wildly, which is a significant problem with this model.

However, the biggest problem with the mass-dependent model is the IMFs shown in Fig. 6, which are very different from the canonical IMFs, as they no longer have a self-similar mapping from the CMF. There is a strong overabundance of stars around the average BE mass in both the single star and the system IMF (though it is more pronounced in the single-star IMF), appearing as a very large ‘bump’ at the peak of this IMF at $\sim 1 M_\odot$. This ‘bump’ is smoothed out somewhat if the SFE is allowed to vary, but is still very distinct. The IMFs tend to decline far too quickly above and below the peak, and the shape is fundamentally wrong (this was noted in passing by Goodwin et al. 2008).

These models are for a range of BE masses chosen core by core. In a scenario for star formation within a single star-forming region, we would expect the BE to be roughly fixed. For a fixed BE mass, the bump is even sharper and more pronounced due to the much stronger mass dependence, and peaks at the value of the BE mass used. This would suggest that the IMF should vary strongly from region to region depending on the local BE mass, which is at odds with the apparent universality of the IMF.

It would be possible to fine-tune this model, e.g. the instantaneously observed form of the CMF does not match the reservoirs of gas available to make stars, and the ‘true’ CMF has a form such that it does map onto the IMF. However, the true CMF would have to have a very particular form that varied in exactly the right way from region to region to then always produce the same, smooth IMF everywhere (we return to this point in the Discussion section).

4.3 Hybrid model

We have shown in Sections 4.1 and 4.2 that core fragmentation struggles to match the observations if it is either completely self-similar or a strong function of core mass. The former cannot reproduce the observed MFs, and the latter produces strange, bumpy, and variable IMFs.

It is plausible that a hybrid model with elements of both previous models might ‘average out’ the problems with each and give an answer that looks like the observations. We therefore consider a model where N_* depends loosely on the core mass. We start by splitting the masses from the CMF uniformly in log space, so that we have a mass range corresponding to each value of N_* . Rather than forcing cores of a given mass to only fragment into N_* stars, we select a random value surrounding the corresponding value of N_* . The mass ranges and their corresponding possible N_* values are shown in Fig. 9.

Varying these conditions slightly makes very little difference to the results we present below, and varying them significantly leads to the same problems we have already discussed with self-similar and mass-dependent models.

For our initial test of this model, stars are ejected from systems using the simple secular plus dynamical model as in Sections 4.1 and 4.2.

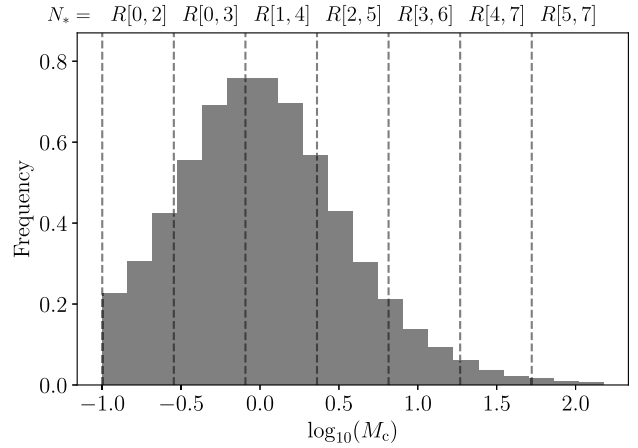


Figure 9. Conditions for fragmentation in the hybrid model. The histogram shows the core mass distribution in log space. The vertical dashed lines show the different mass ranges with the text above each section stating the possible values of N_* (uniformly weighted) for a core in the corresponding mass range.

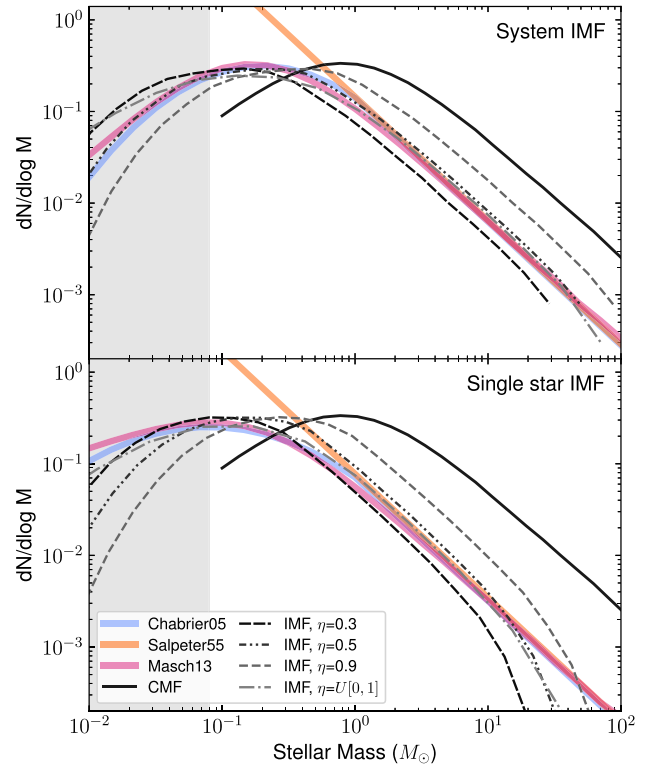


Figure 10. IMFs from the model where core fragmentation is semi-dependent on M_c . See the caption for Fig. 2 for more details.

A hybrid model does provide a better fit to observations as one might expect. In Fig. 10, we can see that the hybrid model fits the system and single-star IMFs reasonably well. The single-star IMF has a very small bump close to the peak, but due to the uncertainties associated with the IMF, the chance of seeing this feature in observations if it exists is unlikely. Furthermore, the high-mass tail of the IMF deviates from the Salpeter slope when $M_p > 20 M_\odot$, but here we are in the low- N tail of our distribution and

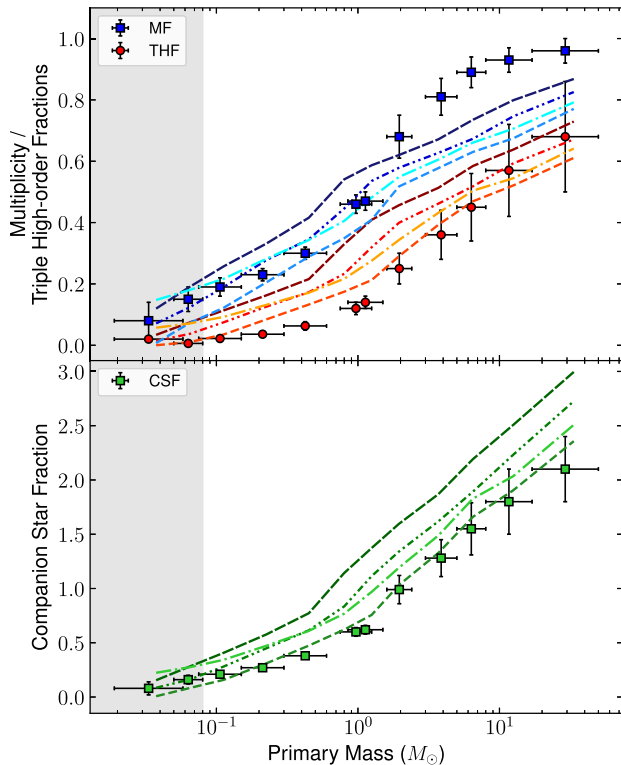


Figure 11. Multiplicities from the model where core fragmentation is semi-dependent on M_c . See the caption for Fig. 2 for more details.

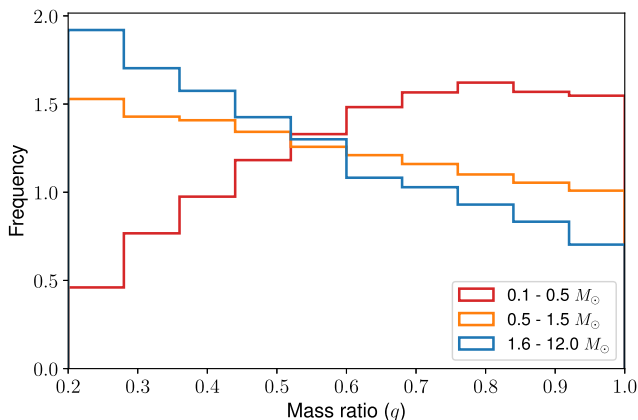


Figure 12. Mass-ratio distributions from the model where core fragmentation is semi-dependent on M_c . See the caption for Fig. 4 for more details.

it is not at all clear whether our universal model would extend to extremely high-mass systems.

The best fits to the different IMFs are at different SFEs: to the system IMF when $\eta = \sim 0.5$. In the case of the single-star IMF, when η is ~ 0.3 . But one could argue that $\eta = 0.4$ would provide a reasonable fit to both IMFs within the observation errors.

In Fig. 11, we see that the hybrid model does a good job of fitting the CSF (green) and THF (red), but is poor at fitting the high-mass end of the MF (blue). In Fig. 12, we see that the mass-ratio distributions do a reasonable job of matching observations: biased to high q for low-mass primaries, roughly flat for solar-mass primaries, and biased to low q for intermediate-mass stars.

The balance of increasing the number of stars formed with core mass, but not fragmenting into so many objects that high-mass stars are underproduced, means that the THFs and CSFs match the observations. However, the MFs for primary stars with masses $> 1 M_\odot$ are far lower than the observations; in the simulated highest mass bin, approximately 60 per cent of stars are in multiples and 50 per cent are in high-order systems, meaning that there are far too many single high-mass stars (compared to the expected number of binaries) in this simulation.

This is due to the large number of binary systems that decay due to the random ejection rules in our simulations; most cores massive enough to form stars \geq a few solar masses will form a large number of stars, as in the BE mass-dependent model. The majority of these very high order systems ($N_* = 5-7$) will eject a few stars, diluting the MF whilst keeping the THF and CSF high.

4.3.1 Modelling secular decay only

The models presented above are able to fit various aspects of both the IMFs and multiplicities. However, there are still some major issues with the MFs, which could well be due to our crude model for ejections.

To investigate this, we use the same fragmentation conditions as in Section 4.3, but apply the ejection rules determined by Sterzik & Durisen (1998). They used numerical and analytical modelling of non-hierarchical $N = 3, 4$, and 5 systems to evaluate decay probabilities for secular decay only, which are presented for various initial mass-ratio distributions in their table 1.

As well as considering cases where the multiple system ejects single stars, they also include the various decay channels that produce two lower order systems (i.e. an $N = 5$ system may decay to a binary and a triple system). They do not include any decay statistics for $N = 6$ or $N = 7$ systems, so we extrapolate from the data presented in their paper to estimate the probabilities of high-order systems decaying through each channel (shown in Table 1). We assume that all binaries are stable in this model as it considers secular decay only.

The IMF and MFs determined using the Sterzik & Durisen (1998) decay rules are shown in Figs 13 and 14. The shape of the single-star IMF is the same as in Fig. 10, and the system IMFs are extremely similar as one would expect.

The multiplicity measures are rather different as we have only included secular decay. The MFs (blue) fit well at high masses, but we have far too many multiples at low masses. The THF (red) fits well at all masses, and the CSF (green) is much flatter than the observations. The reasons behind this are worth exploring to see if later dynamical destruction could solve them.

With secular decay only, any binaries survive. At $< 1 M_\odot$ we only have singles, binaries, and triples initially. Most triples will secularly decay to a binary and a single, ejecting the lowest mass member. This reduces the MF, and significantly lowers the THF and CSF as there are so many low-mass single stars and only binaries to counter these. For primaries $> 1 M_\odot$ the initial population contains many triples, quadruples, and even higher order systems. These eject low-mass members (further diluting the multiplicities at lower masses), but retain the highest mass members in binaries and triples resulting in high THFs and CSFs.

Where the secular decay only model fails is to overproduce binaries at lower masses.

A downturn appears in the MF at $0.5-1 M_\odot$ (depending on the SFE). For the best-fitting SFE of $0.3-0.5$, the downturn occurs for primaries less massive than about $\sim 0.7 M_\odot$. The reason for this

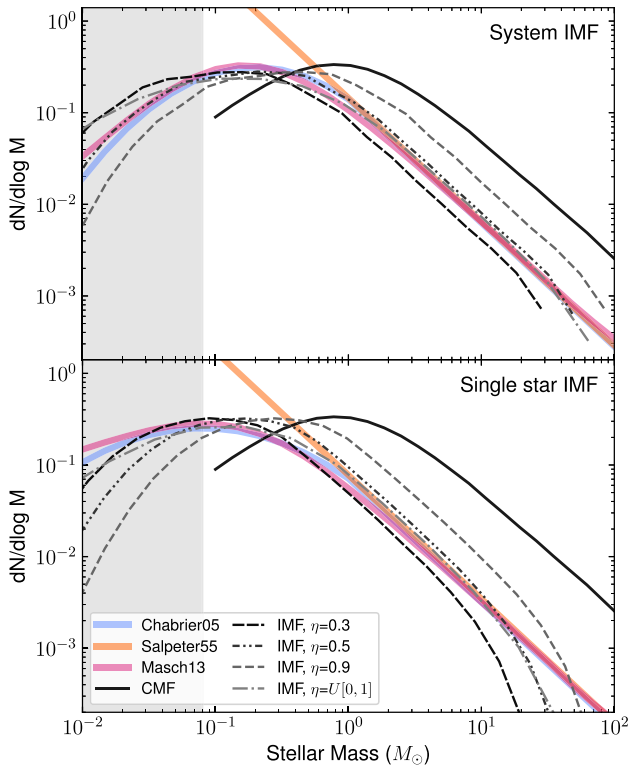


Figure 13. IMFs from the semirandom fragmentation model where low-mass stars are ejected from multiple systems following the Sterzik & Durisen (1998) decay rules. See the caption for Fig. 2 for more details.

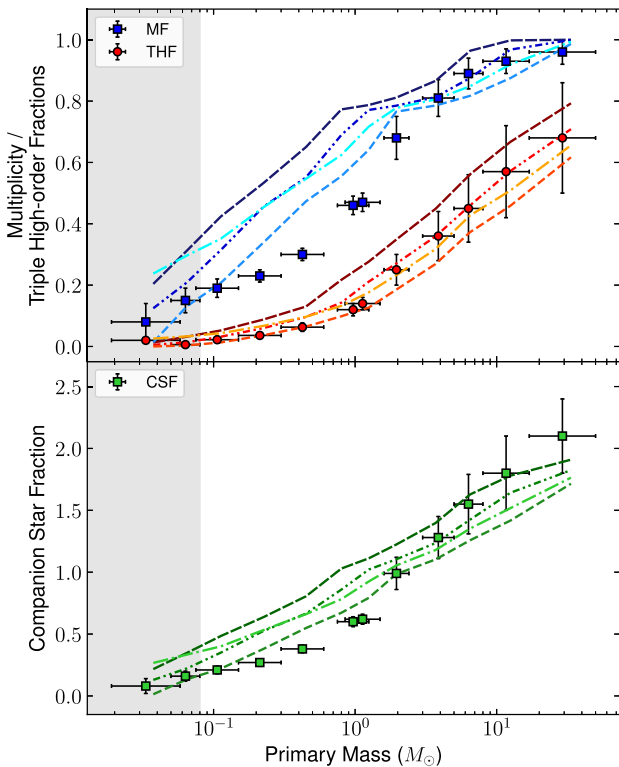


Figure 14. Multiplicities from the semirandom fragmentation model where low-mass stars are ejected from multiple systems following the Sterzik & Durisen (1998) decay rules. See the caption for Fig. 3 for more details.

feature is that systems that form from cores around the peak of the CMF ($\sim 1 M_{\odot}$) will usually form stars of $0.1\text{--}0.5 M_{\odot}$ (one to three stars of total system mass $0.3\text{--}0.5 M_{\odot}$). Therefore by far the most common triple systems around the peak of the IMF will eject stars of typically $0.1\text{--}0.2 M_{\odot}$, which significantly dilutes the lowest mass bins. To dilute mass bins greater than about $0.8 M_{\odot}$ requires ejections of stars of that mass from what must be initially much higher mass cores, which are much rarer.

There are very few systems in which the lowest mass component is about $0.5\text{--}1 M_{\odot}$ and so it is impossible to significantly dilute the MF above that mass. As the system IMF drops to higher masses there are fewer and fewer increasingly high-mass stars ejected to dilute the high-mass MF.

That the observed IMF peaks well below $1 M_{\odot}$ means that the observed rapid decline in MFs between 5 and $0.5 M_{\odot}$ cannot be due to dilution of the MF by secular decay; there are not enough systems with masses greater than a few M_{\odot} that can produce the numbers of ejected roughly solar-mass stars required.

Given our argument in Section 4.2 we cannot enforce a strong change of fragmentation in this regime to cause this rapid change in MF without losing the mapping of the CMF to the IMF. This leaves us with seemingly one option – that additional dynamical decay reduces the MF at low masses to what we observe in the field. We will return to this point in the Discussion section.

5 DISCUSSION

Comparing the IMFs and multiplicities generated from our Monte Carlo simulations to observations allows us to eliminate some universal star formation models.

First, self-similar fragmentation cannot replicate the significant and rapid increase of multiplicity with primary mass. This is because if all cores fragment in the same way, then initially all the multiplicity measures at all masses are equally high. Secular decay will only have a slight mass-dependent effect (preferentially losing the lowest mass members). The only solution would be to have an extremely mass-dependent dynamical decay that destroys almost all low-mass multiples, but having no effect on moderately high-mass multiples. Such a solution would be very fine-tuned and is difficult to see how it could work with a wide variety of different star-forming environments (in particular, in associations there should be very little dynamical decay).

Secondly, having a strict rule where the number of stars formed is proportional to the core mass (in our case, the number of BE masses contained within the core) significantly changes the peak and shape of the IMF. When splitting cores based on a strongly mass-dependent condition, the resulting IMF is a convolution of the CMF and the function defining how N_* depends on M_c , making self-similar mapping impossible.

Given these problems, we tried a hybrid model where core fragmentation is a weak function of core mass. The hybrid model provides a reasonable fit to both the system and single-star IMFs. The gentle dependence of N_* on M_c solves the problem of overproducing low-mass multiples (as in the self-similar model) without introducing harsh features in the IMF (as in the strongly core mass-dependent model).

However, the hybrid model is not perfect. Its main problem is that it really struggles in overproducing binaries for primaries $< 2 M_{\odot}$ (see the top panel of Fig. 14). In smoothing the mass dependence of fragmentation to keep the IMF close to observations, it fails to give the quite rapid decline in MF that we observe. However, if we change the fragmentation rule to optimize fitting the MFs, then this breaks

the smoothness of the IMF in regions away from the peak of the IMF (around $1 M_{\odot}$). It is better than the self-similar model in its fit to the multiplicities, but in some ways retains the same fundamental problem.

We have been unable to find a simple rule for the conversion of a static CMF to multiple systems that is able to fit the observations of both a universal canonical IMF and the multiplicities of the field.

One possible reason is that no such rule exists, and star formation is not universal and that different regions produce at least different multiplicity properties (and perhaps slightly different IMFs). The field would therefore just be the average of these different star formation events. This would solve our problem, but at the cost of making every star formation event potentially quite different in its outcomes, and so there is no single answer to the question ‘How do stars form?’ (and so no single ‘right answer’ to compare simulations to).

Another possibility is that the observed CMF does not represent a static distribution of the mass reservoirs available to form stars. We are assuming that a core mass remains constant and therefore a $1 M_{\odot}$ core contains $1 M_{\odot}$ of gas from which it can form stars. However, cores should (at least sometimes) be able to accrete more mass, and so the mass of a core at the instant it is observed is not a measure of how much mass will be available to form stars. This would mean that we are not using the ‘correct’ CMF as a starting point. Whilst this would allow us to vary the CMF from what is observed, it is not obvious to what extent this would change the results of our models. We are already in some way accounting for this in having variable SFEs, as we already assume that not all the gas in a core will turn into stellar mass – so if the core mass grows this can be accounted for within the SFE. However, we are still left with the problem that the CMF would need to have an unusual shape to balance out the feature at $\sim 1 M_{\odot}$, introduced by the strongly mass-dependent fragmentation model. First, there is no reasoning that we can see which would explain why the CMF should have exactly the form required to produce a nice, smooth resulting IMF. Secondly, if where fragmentation occurs changes with the environment (e.g. varying Bonner–Ebert masses), then the CMF would need to be altered in each region in such a way as to produce the same smooth canonical IMF everywhere.

Throughout, we have assumed that the IMF is universal, and have judged the quality of fit of our simulations similarities to the canonical IMF. Whilst this is widely assumed, there is still some debate about the level of variation between IMFs in different regions. Observations of young clusters by Dib (2014) suggest that the IMF may not be universal, but there is also strong evidence that the form of the IMF is mostly unaffected by environmental factors (Damian et al. 2021; Guszejnov et al. 2022). Interestingly, the strongly peaked IMF as seen in our mass-dependent model shows some similarities to the unusual IMF in Taurus (Luhman et al. 2003; Dib 2014), which has a strong peak at $\sim 0.8 M_{\odot}$. A detailed comparison between our simulated IMF and the observed IMF in Taurus is outside the scope of this paper, but similarities are intriguing (cf. Goodwin et al. 2004).

5.1 Secular and dynamical decay modelling

The secular and dynamical decay conditions we applied to the models are a simplified version of the physical processes occurring during star formation. We applied the decay probabilities of Sterzik & Durisen (1998) to see what purely secular decay would do to the hybrid model. We find that it fits the multiplicity properties for primaries greater than $2 M_{\odot}$ surprisingly well, but results in too many binaries (not triples or higher order systems) for primaries of $0.1\text{--}2 M_{\odot}$. The MF does decline with primary mass in this range, but

is consistently roughly double the field values for all primary masses in this range.

There are two interesting things to say about this result.

First, as we mentioned above, in order to fit the field multiplicities we would need to dynamically process some of these binaries into two singles. In order to reduce the MF by a factor of 2, we need to dynamically destroy about a third of the systems. For example, for an MF of 0.6, i.e. 60/100, to become an MF of 0.3, if we process 20 of the 60 binaries into 40 singles the MF is now 40/120 (lowering the number of binaries from 60 to 40, and in the process producing 20 new single systems). This would need to be somewhat mass dependent: not effective for systems with primaries over a few M_{\odot} , and equally effective for all low-mass systems.

This is still quite a significant level of processing that requires one-third of systems to spend enough time in an environment with high enough density and encounter energy to have an unbinding encounter. However, one-third of systems spending time in such an environment (e.g. a fairly dense cluster) is not implausible, and such environments are effective at processing binaries (e.g. Parker et al. 2009).

Secondly, a slight overabundance of binaries is observed in some local star-forming regions. King et al. (2012a, b) found that local low-density star-forming regions all show a similar overabundance of multiples by a factor of roughly 2 when compared to the field, and Duchêne et al. (2018) find the same overabundance in the Orion Nebula Cluster. Therefore, for at least roughly $1 M_{\odot}$ primaries local star-forming regions possibly match the too high MFs found with secular decay only in the hybrid model. This might possibly argue for the hybrid model being a good model of how cores produce stellar systems, and then how those systems secularly decay.

A problem here is that the observed local overabundance contains too many hard binaries below 100 au separation to be dynamically processed by any of the environments in which they are found (King et al. 2012a, b; Duchêne et al. 2018).

Therefore, we would require around one-third of stars to be formed at much higher densities than we observe locally in order to process them. This could cause problems to the universal model we are trying to make work in this paper as then it is arguable that they do not form in the same way as stars locally. In particular, at high densities cores will not be isolated while forming stars and they will interact (Goodwin et al. 2007), and we have implicitly assumed cores are isolated objects so that there can be a mapping from the CMF to IMF. Since locally we observe cores to be quite separate, isolated objects, this could suggest a different ‘mode’ of forming stars in much denser environments.

5.2 Inclusion of brown dwarf companions

As mentioned in Section 3, we include all companions with a mass $>0.012 M_{\odot}$ (the minimum brown dwarf mass) in our multiplicity statistics. The solar-type MFs are calculated by counting all stellar and brown dwarf companions (Raghavan et al. 2010), but the original M dwarf statistics from Winters et al. (2019) do not include brown dwarf companions; in a discussion of results, however, they state that the inclusion of BD companions only increases the MFs by ~ 1 per cent. For intermediate/higher mass stars, the surveys by De Rosa et al. (2014) ($1.6\text{--}2.4 M_{\odot}$), Moe & Kratter (2021) ($1.6\text{--}2.4 M_{\odot}$), and Moe & Di Stefano (2017) ($3\text{--}17 M_{\odot}$) identified companions down to $0.08 M_{\odot}$, and only corrected for completeness down to this limit. Furthermore, the majority of MFs are calculated for different separation distributions, which were factored into our simulations.

5.3 Separation distributions

There are several additional factors that could be taken into account in order to make this model more detailed. Applying a mask of different separations to each of our multiple systems would allow us to predict the MFs across different separation ranges and compare these results to observations. We could also use the separation distribution to estimate which systems would be detected in observational surveys, which would then allow us to introduce a new model for the dynamic and secular decay of systems depending on the separations. Incorporating these effects would contravene the main purpose of our simulations (to find a simple rule that reproduces the overall multiplicity trend with mass), but would provide interesting opportunities for follow-up research.

5.4 Comparisons to previous statistical studies

Star formation from molecular cores is not a trivial process to model. Turbulence, magnetic fields, rotation, and chemistry (among other properties) all need to be taken into account for detailed simulations of multiple system formation.

Previous statistical models have had success in reproducing some of the observed multiplicity and properties and stellar IMF of different populations of stars. Recent simulation works by Guszejnov & Hopkins (2015), Guszejnov et al. (2017), and Haugbølle, Padoan & Nordlund (2018) predict that the observed IMF and MFs are predominantly set by isothermal turbulence, in agreement with past simulations such as Goodwin et al. (2004). Guszejnov et al. (2017) model star formation from the beginning of the GMC collapse and predict properties such as the spatial distribution of the stars, which our simulations do not. We also note that Guszejnov et al. (2023) and Kuruwita & Haugbølle (2023) have had success numerically reproducing the field MFs with core fragmentation-only models.

We also note that Ambrose & Whitworth (in preparation) have had success in reproducing the MF of solar-type stars using an N -body model of secular decay only.

Our simulations complement the results of past studies by comparing results to the THF and CSF, which are not quantified in studies such as Holman et al. (2013) or Guszejnov et al. (2017). Furthermore, the aims of our models differ from those of more physically detailed hydrodynamical or semi-analytical models, as we are aiming to explore the universality of star formation using simple rules, and focusing on the dependence of the IMF and multiplicities primarily on core mass.

6 CONCLUSIONS

We have tested several scenarios for universal star formation. Using the stellar populations at the end of the simulation, we have compared our results to the observed IMF and MFs of the field. We have not found a model that perfectly fits both the IMF and multiplicities, but some models have more success than others.

The key issue with self-similar fragmentation, in which all cores form a random number of stars irrespective of the initial core mass, is that it produces MFs that do not have the strong primary mass dependence seen in the observations. If cores fragment with a strong dependence on their mass, this breaks the self-similar mapping between the CMF and the IMF, and produces a significant feature in the IMF around the peak.

A hybrid model with a weak core mass fragmentation dependence finds a good fit to the IMF, and a somewhat reasonable fit to the

multiplicities. Interestingly, the hybrid model with secular decay only seems to match the IMF and multiplicities of local star-forming regions, but it appears non-trivial to argue for how those multiplicities could be processed to form the field.

ACKNOWLEDGEMENTS

We thank the anonymous referee for the helpful feedback that improved the quality of this work. RJH acknowledges support from the UK Science and Technology Facilities Council in the form of a PhD studentship. For the purpose of open access, the author has applied a CC BY public copyright licence to any Author Accepted Manuscript version arising.

DATA AVAILABILITY

All data underlying this article will be shared upon reasonable request.

REFERENCES

- Alves J., Lombardi M., Lada C. J., 2007, *A&A*, 462, L17
 André P. et al., 2010, *A&A*, 518, L102
 Anosova J. P., 1986, *Ap&SS*, 124, 217
 Attwood R. E., Goodwin S. P., Stamatellos D., Whitworth A. P., 2009, *A&A*, 495, 201
 Bastian N., Covey K. R., Meyer M. R., 2010, *ARA&A*, 48, 339
 Bate M. R., 2012, *MNRAS*, 419, 3115
 Benson P. J., Myers P. C., 1989, *ApJS*, 71, 89
 Bonnell I. A., Bate M. R., 2006, *MNRAS*, 370, 488
 Bonnell I. A., Larson R. B., Zinnecker H., 2007, in Reipurth B., Jewitt D., Keil K., eds, *Protostars and Planets V*. Univ. Arizona Press, Tucson, AZ, p. 149
 Bonnor W. B., 1956, *MNRAS*, 116, 351
 Chabrier G., 2003, *PASP*, 115, 763
 Chen C.-Y., Mundy L. G., Ostriker E. C., Storm S., Dhabal A., 2020, *MNRAS*, 494, 3675
 Damjan B., Jose J., Samal M. R., Moraux E., Das S. R., Patra S., 2021, *MNRAS*, 504, 2557
 Deacon N. R., Kraus A. L., 2020, *MNRAS*, 496, 5176
 Delgado-Donate E. J., Clarke C. J., Bate M. R., 2003, *MNRAS*, 342, 926
 De Rosa R. J. et al., 2014, *MNRAS*, 437, 1216
 Dib S., 2014, *MNRAS*, 444, 1957
 Duchêne G., 1999, *A&A*, 341, 547
 Duchêne G., Kraus A., 2013, *ARA&A*, 51, 269
 Duchêne G., Lacour S., Moraux E., Goodwin S., Bouvier J., 2018, *MNRAS*, 478, 1825
 Duquennoy A., Mayor M., 1991, *A&A*, 248, 485
 Ebert R., 1955, *Z. Astrophys.*, 37, 217
 Fischer D. A., Marcy G. W., 1992, *ApJ*, 396, 178
 Goodwin S. P., 2010, *Phil. Trans. R. Soc. A*, 368, 851
 Goodwin S. P., 2013, *MNRAS*, 430, L6
 Goodwin S. P., Kroupa P., 2005, *A&A*, 439, 565
 Goodwin S. P., Whitworth A. P., Ward-Thompson D., 2004, *A&A*, 419, 543
 Goodwin S. P., Kroupa P., Goodman A., Burkert A., 2007, in Reipurth B., Jewitt D., Keil K., eds, *Protostars and Planets V*. Univ. Arizona Press, Tucson, AZ, p. 133
 Goodwin S. P., Nutter D., Kroupa P., Ward-Thompson D., Whitworth A. P., 2008, *A&A*, 477, 823
 Guszejnov D., Hopkins P. F., 2015, *MNRAS*, 450, 4137
 Guszejnov D., Hopkins P. F., Krumholz M. R., 2017, *MNRAS*, 468, 4093
 Guszejnov D., Grudić M. Y., Offner S. S. R., Faucher-Giguère C.-A., Hopkins P. F., Rosen A. L., 2022, *MNRAS*, 515, 4929
 Guszejnov D., Raju A. N., Offner S. S. R., Grudić M. Y., Faucher-Giguère C.-A., Hopkins P. F., Rosen A. L., 2023, *MNRAS*, 518, 4693
 Haisch K. E., Jr, Greene T. P., Barsony M., Stahler S. W., 2004, *AJ*, 127, 1747

- Haugbølle T., Padoan P., Nordlund Å., 2018, *ApJ*, 854, 35
- Hennebelle P., Chabrier G., 2008, *ApJ*, 684, 395
- Holman K., Walch S. K., Goodwin S. P., Whitworth A. P., 2013, *MNRAS*, 432, 3534
- Hurley J. R., Aarseth S. J., Shara M. M., 2007, *ApJ*, 665, 707
- King R. R., Parker R. J., Patience J., Goodwin S. P., 2012a, *MNRAS*, 421, 2025
- King R. R., Goodwin S. P., Parker R. J., Patience J., 2012b, *MNRAS*, 427, 2636
- Könyves V. et al., 2010, *A&A*, 518, L106
- Könyves V. et al., 2015, *A&A*, 584, A91
- Könyves V. et al., 2020, *A&A*, 635, A34
- Kratter K., Lodato G., 2016, *ARA&A*, 54, 271
- Kraus A. L., Ireland M. J., Martinache F., Hillenbrand L. A., 2011, *ApJ*, 731, 8
- Kroupa P., 1995a, *MNRAS*, 277, 1491
- Kroupa P., 1995b, *MNRAS*, 277, 1522
- Kroupa P., 2001, *MNRAS*, 322, 231
- Kroupa P., Bouvier J., 2003, *MNRAS*, 346, 343
- Kroupa P., Weidner C., Pflamm-Altenburg J., Thies I., Dabringhausen J., Marks M., Maschberger T., 2013, in Oswalt T. D., Gilmore G., eds, *Planets, Stars and Stellar Systems. Vol. 5: Galactic Structure and Stellar Populations*. Springer, Dordrecht, p. 115
- Kuruwita R. L., Haugbølle T., 2023, *A&A*, 674, A196
- Lada C. J., Muench A. A., Rathborne J., Alves J. F., Lombardi M., 2008, *ApJ*, 672, 410
- Leinert C., Zinnecker H., Weitzel N., Christou J., Ridgway S. T., Jameson R., Haas M., Lenzen R., 1993, *A&A*, 278, 129
- Lomax O., Whitworth A. P., Hubber D. A., Stamatellos D., Walch S., 2015, *MNRAS*, 447, 1550
- Luhman K. L., Briceño C., Stauffer J. R., Hartmann L., Barrado y Navascués D., Caldwell N., 2003, *ApJ*, 590, 348
- Marsh K. A. et al., 2016, *MNRAS*, 459, 342
- Maschberger T., 2013, *MNRAS*, 429, 1725
- Mason B. D., Hartkopf W. I., Gies D. R., Henry T. J., Helsel J. W., 2009, *AJ*, 137, 3358
- Massi F. et al., 2019, *A&A*, 628, A110
- Matzner C. D., McKee C. F., 2000, *ApJ*, 545, 364
- Moe M., Di Stefano R., 2017, *ApJS*, 230, 15
- Moe M., Kratter K. M., 2021, *MNRAS*, 507, 3593
- Motte F., Andre P., Neri R., 1998, *A&A*, 336, 150
- Nony T. et al., 2023, *A&A*, 674, A75
- Nutter D., Ward-Thompson D., 2007, *MNRAS*, 374, 1413
- Offner S. S. R., Clark P. C., Hennebelle P., Bastian N., Bate M. R., Hopkins P. F., Moraux E., Whitworth A. P., 2014, in Beuther H., Klessen R. S., Dullemond C. P., Henning T., eds, *Protostars and Planets VI*. Univ. Arizona Press, Tucson, AZ, p. 53
- Offner S. S. R., Moe M., Kratter K. M., Sadavoy S. I., Jensen E. L. N., Tobin J. J., 2023, in Inutsuka S.-i., Aikawa Y., Muto T., Tomida K., Tamura M., eds, *ASP Conf. Ser. Vol. 534, Protostars and Planets VII*. Astron. Soc. Pac., San Francisco, p. 275
- Padoan P., Nordlund Å., 2002, *ApJ*, 576, 870
- Parker R. J., Goodwin S. P., 2012, *MNRAS*, 424, 272
- Parker R. J., Goodwin S. P., Kroupa P., Kouwenhoven M. B. N., 2009, *MNRAS*, 397, 1577
- Patience J., Ghez A. M., Reid I. N., Matthews K., 2002, *AJ*, 123, 1570
- Pelkonen V. M., Padoan P., Haugbølle T., Nordlund Å., 2021, *MNRAS*, 504, 1219
- Raghavan D. et al., 2010, *ApJS*, 190, 1
- Rawirawattana K., Goodwin S. P., 2023, *ApJ*, 947, 12
- Reipurth B., Mikkola S., 2012, *Nature*, 492, 221
- Reipurth B., Clarke C. J., Boss A. P., Goodwin S. P., Rodríguez L. F., Stassun K. G., Tokovinin A., Zinnecker H., 2014, in Beuther H., Klessen R. S., Dullemond C. P., Henning T., eds, *Protostars and Planets VI*. Univ. Arizona Press, Tucson, AZ, p. 267
- Sadavoy S. I., Stahler S. W., 2017, *MNRAS*, 469, 3881
- Salpeter E. E., 1955, *ApJ*, 121, 161
- Sana H. et al., 2012, *Science*, 337, 444
- Sana H. et al., 2014, *ApJS*, 215, 15
- Scibelli S., Shirley Y., 2020, *ApJ*, 891, 73
- Sterzik M. F., Durisen R. H., 1998, *A&A*, 339, 95
- Tobin J. J. et al., 2022, *ApJ*, 925, 39
- Tokovinin A., 2014, *AJ*, 147, 87
- Torres G., Latham D. W., Quinn S. N., 2021, *ApJ*, 921, 117
- Valtonen M., Mylläri A., Orlov V., Rubinov A., 2008, in Vesperini E., Giersz M., Sills A., eds, *Proc. IAU Symp. Vol. 246, Dynamical Evolution of Dense Stellar Systems*. Cambridge Univ. Press, Cambridge, p. 209
- Vázquez-Semadeni E., Palau A., Ballesteros-Paredes J., Gómez G. C., Zamora-Avilés M., 2019, *MNRAS*, 490, 3061
- Ward-Duong K. et al., 2015, *MNRAS*, 449, 2618
- Winters J. G. et al., 2019, *AJ*, 157, 216
- Wright N. J., Goodwin S., Jeffries R. D., Kounkel M., Zari E., 2023, in Inutsuka S. i., Aikawa Y., Muto T., Tomida K., Tamura M., eds, *ASP Conf. Ser. Vol. 534, Protostars and Planets VII*. Astron. Soc. Pac., San Francisco, p. 129

This paper has been typeset from a $\text{\TeX}/\text{\LaTeX}$ file prepared by the author.